means of defining an engineering model of the Mars surface wind environment.

Acknowledgment

The author acknowledges the support of the Cassini project.

References

[1]Hess, S. L., Henry, R. M., Leovy, C. B., Ryan, J. A., and Tillman, J. E., "Meteorological Results from the Surface of Mars: Viking 1 and 2," *Journal of Geophysical Research*, Vol. 82, No. 28, 1977, pp. 4559–4574.

[2]Hess, S. L., Henry, R. M., Leovy, C. B., Ryan, J. A., and Tillman, J. E., "Early Meteorological Results from the Viking 2 Lander," *Science*, Vol. 194, No. 17, 1976, pp. 1352, 1353.

[3]Tillman, J. E., Henry, R. M., and Hess, S. L., "Frontal Systems During Passage of the Martian North Polar Hood over the Viking Lander 2 Site Prior to the First 1977 Dust Storm," *Journal of Geophysical Research*, Vol. 84, No. B6, 1979, pp. 2947–2955.

[4]Ryan, J. A., Henry, R. M., Hess, S. L., Leovy, C. B., Tillman, J. E., and Walcek, C., "Mars Meteorology: Three Seasons at the Surface," *Geophysical Research Letters*, Vol. 5, No. 8, 1978, pp. 715–718.

[5]Ojusu, J. O., and Salawu, R. I., "An Evaluation of Wind Energy Potential as a Power Generation Source in Nigeria," *Solar and Wind Technology*, Vol. 7, No. 6, 1990, pp. 663–673.

[6]Som, A. K., and Ragab, F. M., "A Preliminary Study of Wind Power Potential in Bahrain," *Renewable Energy*, Vol. 3, No. 1, 1993, pp. 67–74.

[7]Coelingh, J. P., van Wijk, A. J. N., Cleijne, J. W., and Pleune, R., "Description of the North Sea Wind Climate for Wind Energy Applications," *Journal of Wind Engineering and Industrial Aerodynamics*, Vol. 39, 1992, pp. 221–232.

[8]Exell, R. H. B., "Wind Energy Potential of Thailand," *Solar Energy*, Vol. 35, No. 1, 1985, pp. 3–12.

[9]Darwish, A. S. K., and Sayigh, A. A. M., "Wind Energy Potential in Iraq," *Solar and Wind Technology*, Vol. 5, No. 3, 1988, pp. 215–222.

[10]Steckemetz, B., Wienss, W., Bradbury, B., Pickett, A., Natenbruck, P., and Roumeas, R., "Flight and Impact Dynamics of Landers for Mars Exploration," 44th Congress of the International Astronautical Federation, Paper IAF-93-Q.1.379, Graz, Austria, Oct. 1993.

[11]Haslach, H. W., "Wind Energy: A Resource for a Human Mission to Mars," *Journal of the British Interplanetary Society*, Vol. 42, 1989, pp. 171–178.

[12]Lorenz, R. D., Lunine, J. I., Grier, J. A., and Fischer, M. A., "Prediction of Aeolian Phenomena on Planets: Application to Titan Paleoclimatology," *Journal of Geophysical Research*, Vol. 100, No. E12, 1995, pp. 26,377–26,386.

A. Tribble
Associate Editor

Navier–Stokes Calculations for Rotating Configurations: Implementation for Rockets

Sara Yaniv*
Israel Military Industries, Ltd.,
Ramat-Hasharon 47100, Israel

Nomenclature

b_{x_i}	= heat flux
H	= total enthalpy
p	= pressure
(u, v, w)	= Cartesian velocity
(x, y, z)	= Cartesian coordinates
ρ	= density
$\tau_{x_i x_j}$	= shear stresses
Ω	= rotating rate
Ω_{ref}	= reference value of rotating rate

Received Sept. 16, 1995; revision received April 2, 1996; accepted for publication May 3, 1996.

*Senior Scientist, Rocket System Division, Department 66/11, P.O.B. 1044.

Introduction

MANY rockets are stabilized by spinning generated by their fins. Among the aerodynamic coefficients needed for flight simulation is the rolling moment coefficient. The rolling moment contains two terms; the forcing term, which is induced by the fins for a nonspinning configuration, and a damping term, which is a dynamic term arising because of spinning. In Ref. 1 the capability to predict the equilibrium spin rate, and the forcing and damping rolling moments for the M829 projectile using a parabolized Navier–Stokes computational code, is reported.

Our primary goal is to derive the forcing and damping rolling moments and to find the rotation rate of the rocket for a given velocity. The forcing rolling moment was calculated for a nonspinning rocket for nonzero angles of attack. Good results as compared with wind-tunnel tests are shown. For a rotating configuration, only zero angle of attack is considered. The flow is periodic and the computations are performed only on one-quarter of the space. For the nonzero angle-of-attack case the flow is not symmetric and the calculations are performed on the whole space with no rotation. For a rotating configuration the flow is generally time dependent. For zero angle of attack, when the Navier–Stokes equations are formulated in a rotating coordinate system with constant rotation rate, the solution is steady state. In this Note, the transonic and supersonic flowfield about rockets with wrap around fins having a small differential cant angle is calculated by solving the three-dimensional Navier–Stokes equations in a rotating system.

The total rolling moment calculated for the rotating configuration contains both the forcing and damping terms. The rolling moment obtained for a rotating configuration is a monotonic function of the rotation rate. The rotation rate at which the rolling moment vanishes indicates the equilibrium rotation rate of a free rocket for a given velocity along its trajectory. Comparison of the calculated rotation rates and those measured in flight tests show very good results.

Governing Equations

The compressible Reynolds averaged Navier–Stokes equations are formulated in a Cartesian reference frame rotating with constant angular velocity Ω around the main rocket axis. For the flow variables, relative to the body rotation, the far-field velocity has a circumferential component, which is a function of the distance from the configuration axis; the far-field boundary condition then depends on the location of the far-field boundary. This could cause a loss of accuracy. To avoid this difficulty the equations are recast in the absolute flow variables defined in the inertial system for which the velocity is uniform in the far field. A similar formulation for the Euler equations is obtained in Ref. 2.

The rotating coordinate system (x, y, z) is shown in Fig. 1. The rotational velocity for a configuration rotating about the main axis x with angular velocity Ω is

$$u_\Omega = 0 \qquad v_\Omega = -\Omega z \qquad w_\Omega = \Omega y \tag{1}$$

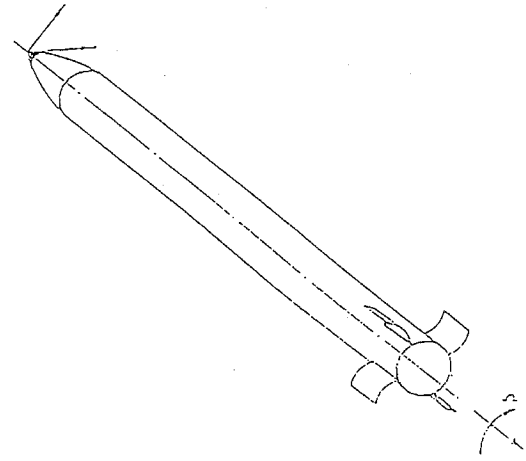

Fig. 1 Typical rocket geometry in a rotating system.

The Navier–Stokes equations for the rotating flow variables are written as follows:

$$\frac{\partial}{\partial t}U + \frac{\partial}{\partial x}F + \frac{\partial}{\partial y}G + \frac{\partial}{\partial z}Q = R \tag{2}$$

where

$$U = \begin{bmatrix} \rho \\ \rho u_r \\ \rho v_r \\ \rho w_r \\ \rho e \end{bmatrix} \tag{3}$$

and

$$\begin{aligned} F &= F^i - F^v \\ G &= G^i - F^v \\ Q &= Q^i - Q^v \end{aligned} \tag{4}$$

The superscript i indicates inviscid and v viscous flux terms;

$$F^i = \begin{bmatrix} \rho u_r \\ \rho u_r^2 + p \\ \rho u_r v_r \\ \rho u_r w_r \\ \rho u_r H \end{bmatrix}; \quad G^i = \begin{bmatrix} \rho v_r \\ \rho u_r v_r \\ \rho v_r^2 + p \\ \rho v_r w_r \\ \rho v_r H \end{bmatrix}; \quad F^i = \begin{bmatrix} \rho w_r \\ \rho u_r w_r \\ \rho w_r v_r \\ \rho w_r^2 + p \\ \rho w_r H \end{bmatrix} \tag{5}$$

and

$$R = \begin{bmatrix} 0 \\ 0 \\ \rho\Omega^2 y - 2\rho\Omega w_r \\ \rho\Omega^2 z + 2\rho\Omega u_r \\ 0 \end{bmatrix} \tag{6}$$

The viscous terms are

$$\begin{aligned} F^v &= [0, \tau_{xx}, \tau_{xy}, \lambda_{xz}, b_x]^T \\ G^v &= [0, \tau_{xy}, \tau_{yy}, \lambda_{yz}, b_y]^T \\ H^v &= [0, \tau_{zx}, \tau_{zy}, \lambda_{zz}, b_z]^T \end{aligned} \tag{7}$$

The turbulence model used as a closure scheme of the Reynolds averaged Navier–Stokes equations is the algebraic turbulence model of Baldwin–Lomax.

Recasting Eq. (2) in terms of absolute velocity components (u, v, w) gives

$$\frac{\partial}{\partial t}\bar{U} + \frac{\partial}{\partial x}\bar{F} + \frac{\partial}{\partial y}\bar{G} + \frac{\partial}{\partial z}\bar{Q} + v_\Omega\frac{\partial \bar{U}}{\partial y} + w_\Omega\frac{\partial \bar{U}}{\partial z} = \bar{R} \tag{8}$$

where

$$U = \begin{bmatrix} \rho \\ \rho u \\ \rho v \\ \rho w \\ \rho e \end{bmatrix}$$

$\bar{F}$, $\bar{G}$, $\bar{Q}$ are the same flux functions of the absolute variables as F, G, Q are for the relative variables, and

$$\bar{R} = \begin{bmatrix} 0 \\ 0 \\ -\rho\Omega w \\ \rho\Omega v \\ 0 \end{bmatrix} \tag{9}$$

The viscous terms, written in the absolute flow variables, remain unchanged.

Numerical Algorithm

A semidiscrete finite volume algorithm based on Jameson's Runge–Kutta time stepping scheme using central differences with artificial viscosity[3–6] is used for obtaining steady-state solutions for the flow variables in the rotating system. We write the convective and diffusive terms in an explicit form and the source term $\bar{R}$ in an implicit form. The source term is

$$\bar{R}^{(n+1)} = \begin{bmatrix} 0 \\ 0 \\ -\Omega(\rho w)^{(n+1)} \\ \Omega(\rho v)^{(n+1)} \\ 0 \end{bmatrix}$$

The implicit equations have the following form:

$$\rho^{(n+1)} = \rho^{(n)} - D(\Psi^1) \tag{10a}$$

$$(\rho u)^{(n+1)} = (\rho u)^{(n)} - D(\Psi^2) \tag{10b}$$

$$(\rho v)^{(n+1)} = (\rho v)^{(n)} - D(\Psi^3) - \Omega \cdot \Delta t \cdot (\rho w)^{(n+1)} \tag{10c}$$

$$(\rho w)^{(n+1)} = (\rho w)^{(n)} - D(\Psi^4) + \Omega \cdot \Delta t \cdot (\rho v)^{(n+1)} \tag{10d}$$

$$(\rho e)^{(n+1)} = (\rho e)^{(n)} - D(\Psi^5) \tag{10e}$$

where $D\Psi^l$, $l = 1, \ldots, 5$, are the flux balance values for each cell.

Equations (10c) and (10d) are solved directly, so that

$$(\rho v)^{(n+1)} = \frac{(\rho v)^{(n)} - \Delta\Psi^3 - \Omega \cdot \Delta t \cdot \left[(\rho w)^{(n)} - \Delta\Psi^4\right]}{[1 + (\Omega \cdot \Delta t)^2]} \tag{10c'}$$

$$(\rho w)^{(n+1)} = \frac{(\rho w)^{(n)} - \Delta\Psi^4 - \Omega \cdot \Delta t \cdot \left[(\rho v)^{(n)} - \Delta\Psi^3\right]}{[1 + (\Omega \cdot \Delta t)^2]} \tag{10d'}$$

Equations (10c') and (10d') replace Eqs. (10c) and (10d) in the difference scheme.

Boundary Conditions

The far-field boundary conditions for the absolute flow variables are applied at a finite distance from the body using Riemann invariants in the direction normal to the outer boundary.[4] The no slip boundary condition for the rotating solid configuration is prescribed as follows: For the rotated axisymmetric body we prescribe the tangential velocity and set the normal velocity to zero. This is applicable only for viscous flow since the Euler equations use only the normal velocity component as a boundary condition. For the fins or any other part of the configuration that is not cylindrical the tangential and normal velocity components are prescribed.

Results

The solutions of the flow about rotating configurations were computed with our multiblock code for the generalized three-dimensional Navier–Stokes equations in the rotating reference frame. The typical aerodynamic configuration is shown in Fig. 1. The body has a large aspect ratio with small wraparound fins having nonzero differential cant angle with the body. For the general case of nonzero angle-of-attack flight, the flow is not symmetric and the whole space is to be solved for the nonrotating case.

For the rotating configuration flying with zero angle of attack the flow is steady in the rotating frame of reference and for the four fin configuration only a quarter of the entire configuration need be modeled. Only one fin with approximately 45 deg of body surface on either side is considered with appropriate periodic boundary conditions at the outer circumferential boundary.

The computational grid consists of six blocks as determined by the configuration. In the circumferential direction the total grid contains 33 grid points for the quarter space. In the longitudinal direction there are 109 points along the whole body, and in the direction normal to the body there are 54 points. A limited grid refinement study

has been conducted. The effect of grid refinement in the circumferential direction is investigated by increasing the number of grid points from 33 to 49. The effect on the rolling moment was very small.

The efficiency of the present scheme is demonstrated by examining the convergence history of the numerical solution. The residual is reduced by 3 orders of magnitude in 800 iterations, and the value of the rolling moment is obtained accurately after only 200 iterations.

Various computations for rockets with wraparound fins having 1-deg cant angle have been performed. Since our code deals with

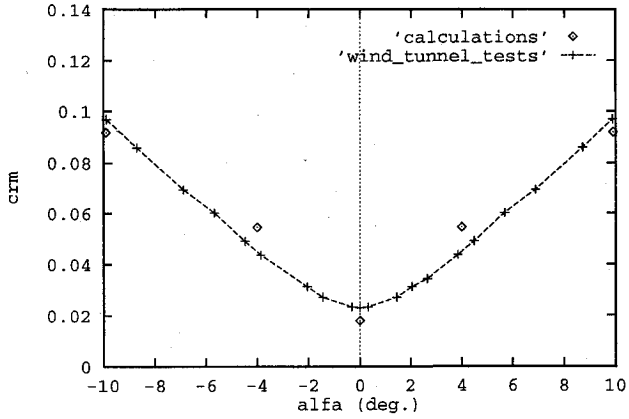

Fig. 2 Forcing roll moment.

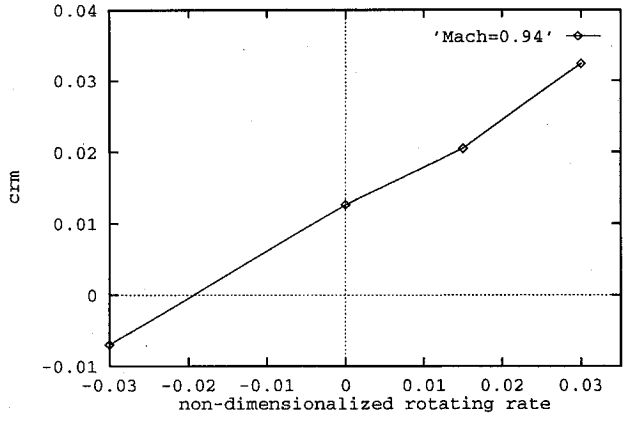

Fig. 3 Total roll moment.

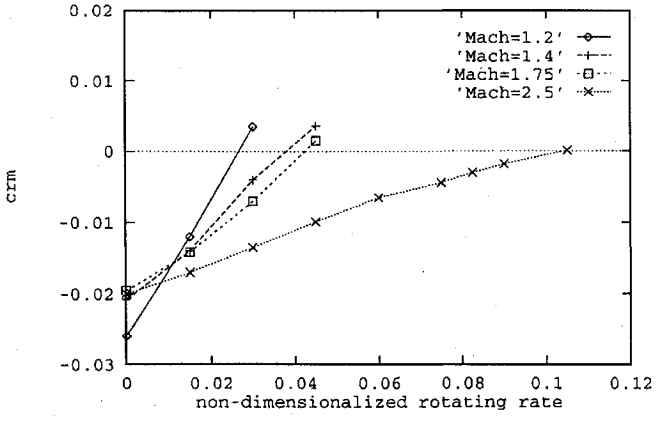

Fig. 4 Total roll moment.

Table 1 Comparison between equilibrium rotating rate of free rocket (obtained from flight tests) and those obtained from computational fluid dynamics calculations

Mach no.	Calculated rotating rates	Flight tests' rotating rates
0.94	8	8.5
1.2	12	10
1.4	16	13
1.75	19	15

nondimensionalized variables, the rotation rate is normalized by the reference value Ω_{ref}. We calculated the forcing rolling moment coefficient as a function of the angle of attack for different Mach numbers. For this case Ω is set to zero. Figure 2 shows the behavior of the forcing rolling moment vs angle of attack for Mach = 1.2 compared with the results obtained in the wind-tunnel tests. Figures 3 and 4 show the total rolling moment as function of the rotation rate for transonic and supersonic speeds.

The nondimensionalized value of Ω for which the total rolling moment is zero, obtained from our calculations, defines the equilibrium rotation rate of the projectile for the momentary speed along its flight. This value is available from flight tests. Table 1 shows the equilibrium rotation rate of the rocket, obtained in flight tests, and those obtained from our computations. A very good comparison is reached.

Conclusions

The three-dimensional Navier–Stokes equations are solved in a rotating coordinate frame of references for the absolute flow variables. The method we use in the study indicates that the rolling moment is calculated correctly for a rocket with wraparound fins flying at transonic and supersonic speeds. For rockets rotating along their trajectory the equilibrium rotating rate is the value of Ω for which the damping rolling moment, added to the forcing rolling moment, gives a zero value for the total rolling moment.

From the calculations of the rolling moment as a function of the angular velocity, the derivative of the rolling moment with respect to the rotation rate is available. This derivative is a significant term in the equations describing rockets' flight.

References

[1]Sturek, W. B., Nietubitz, C. J., Sahu, J., and Weinacht, P., "Recent Applications of CFD to the Aeronautics of Army Projectiles," U.S. Army Research Lab., ARL-TR-22, Aberdeen Proving Ground, MD, Dec. 1992.

[2]Agarwal, R. K., and Deese, J. E., "Euler Calculations for Flowfield of a Helicopter Rotor in Hover," *Journal of Aircraft*, Vol. 24, No. 4, 1987, pp. 231–238.

[3]Jameson, A., Schmidt, W., and Turkel, E., "Numerical Solutions of the Euler Equations by Finite Volume Methods Using Runge–Kutta Time Stepping Schemes," AIAA Paper 81-1259, June 1981.

[4]Jameson, A., and Baker, T. J., "Solution of the Euler Equations for Complex Configurations," AIAA Paper 83-1929, July 1983.

[5]Vatsa, V. N., and Wedan, B. W., "Development of a Multigrid Code for 3-D Navier–Stokes Equations and Its Application to a Grid-Refinement Study," *Computers and Fluids*, Vol. 18, No. 4, 1990, pp. 391–403.

[6]Swanson, R. C., and Turkel, E., "On Central Difference and Upwind Schemes," *Journal of Computational Physics*, Vol. 101, No. 2, 1992, pp. 292–306.

R. M. Cummings
Associate Editor